Chemical Science

ROYAL SOCIETY OF CHEMISTRY

EDGE ARTICLE

View Article Online
View Journal

Cite this: DOI: 10.1039/d6sc03696a

All publication charges for this article have been paid for by the Royal Society of Chemistry

Photochemical post-functionalization of polystyrene enables accelerated chemical recycling

Stanley Lo, [ab] Angela Lin,[a] Cher Tian Ser,[ab] Alán Aspuru-Guzik [*abcdefghi] and Helen Tran [*ade]

Molecular post-modification design strategies that enable low-temperature pyrolysis of polystyrene (PS) remain an underexplored area. Conventional pyrolysis of PS demands heating above 400 °C, creating economic barriers to commercial-scale monomer recovery. Here, we demonstrate the post-functionalization of the PS backbone with a labile C–S bond, specifically a trifluoromethylthio group (–SCF_3), to accelerate the depolymerization of PS at lower temperatures. A previously established small-molecule trifluoromethylthiolation reaction was adapted to PS through solvent screening and reaction optimization. Across a wide range of molecular weights (M_n = 1.12–110 kg mol^{-1}), including consumer-grade samples, thermogravimetric analysis demonstrates that PS-SCF_3 exhibits an onset degradation temperature 10–20 °C lower and a greater mass loss of 10–35% over 20 hours at 300 °C compared to pristine PS. Flynn–Ozawa–Wall analysis reveals that the average apparent activation energy for depolymerization of PS-SCF_3 is approximately 11 kJ mol^{-1} lower than that of pristine PS. To assess the potential industrial relevance of this protocol, pyrolysis of several consumer-grade PS samples and their post-modified PS-SCF_3 analogues was performed at 300 °C; PS-SCF_3 samples were found to afford higher styrene recovery relative to pristine PS. This study explores the potential of backbone post-functionalization of PS as a strategy to accelerate depolymerization at lower temperatures and shorter timescales, enabling greater styrene recovery and advancing progress toward a circular economy for plastics.

Received 1st May 2026
Accepted 15th May 2026

DOI: 10.1039/d6sc03696a

rsc.li/chemical-science

Introduction

Polystyrene (PS) is among the top six globally produced commodity plastics, yet remains one of the least recycled plastics.[1] Pyrolysis is one of the most promising methods for chemical recycling to monomer, where plastics are heated above their ceiling temperature (T_c) under nonequilibrium conditions (*i.e.* depolymerization temperature) and an inert atmosphere to yield monomeric feedstock.[2–4] However, one of the main barriers to the adoption of pyrolysis is the requirement of high temperatures for maintaining efficient depolymerization, making it energy-intensive, expensive, and incompatible with intermittent renewable energy.[5–7] PS remains an underexplored commodity polymer for chemical recycling due to its high T_c of 397 °C;[8] the polymerization of PS is highly exothermic and reversibly, the depolymerization of PS is highly endothermic.[9,10] While depolymerization of PS can be observed at 280 °C over multiple days, conventional pyrolysis of PS typically requires temperatures upward of 400 °C for processing times of 40 minutes to make it commercially relevant.[11–14]

This temperature–time trade-off motivates research efforts towards recycling PS at lower temperatures and/or faster timescales. To accelerate depolymerization at low temperatures, PS depolymerization would necessitate the promotion of *in situ* carbanion or radical generation with an activation energy barrier lower than the homolysis of the polymer backbone.[2,11,12] Marquez *et al.* highlight several examples of using base catalysts to selectively abstract tertiary protons, forming carbanion intermediates that depolymerize preferentially to styrene.[11,13,15] Kumar *et al.* rely on another approach of using cations from various salts to destabilize the PS radical which moderately accelerates depolymerization.[16] Despite the improved styrene recovery achieved by both approaches, the necessary reaction

[a]*Department of Chemistry, University of Toronto, 80 St. George St., Toronto, ON M5S 3H6, Canada. E-mail: aspuru@utoronto.ca; tran@utoronto.ca*
[b]*Vector Institute for Artificial Intelligence, W1140-108 College St., Schwartz Reisman Innovation Campus, Toronto, ON M5G 0C6, Canada*
[c]*Department of Computer Science, University of Toronto, 40 St. George St., Toronto, ON M5S 2E4, Canada*
[d]*Department of Chemical Engineering and Applied Chemistry, University of Toronto, Toronto, ON, M5S 3E5, Canada*
[e]*Acceleration Consortium, 700 University Ave., Toronto, ON M7A 2S4, Canada*
[f]*Department of Materials Science and Engineering, University of Toronto, ON M5S 3E4, Canada*
[g]*Institute of Medical Science, 1 King's College Circle, Medical Sciences Building, Room 2374, Toronto, ON M5S 1A8, Canada*
[h]*Canadian Institute for Advanced Research (CIFAR), 661 University Ave., Toronto, ON M5G 1M1, Canada*
[i]*NVIDIA, 431 King St. W #6th, Toronto, ON M5V 1K4, Canada*

temperatures remain elevated, typically ranging from 350 °C to above 400 °C. An alternative approach by Doucet *et al.* and Oh *et al.* is to add a photon-absorbing material (*i.e.* graphite,[17] or carbon black,[18]) that can localize high temperatures on the surface of the nanoparticles to promote PS depolymerization. More recently, Young *et al.* synthesized a novel copolymer of styrene and an *N*-(methacryloxy)phthalimide that achieved >90% styrene recovery within 2 hours at 290 °C due to the labile N–O bond that improves mid-chain initiation of the polymer backbone.[19] We envision that depolymerization methods to pure monomers can have reduced barriers to adoption if it can be achieved at temperatures lower than 350 °C, and faster timescales.

In this work, we present a photochemical post-functionalization of labile C–S bonds onto the PS backbone that renders lab-grade and consumer-grade PS amenable to low-temperature pyrolysis at 300 °C, recovering styrene in shorter reaction times than conventional thermal depolymerization. Our approach was inspired by Howell *et al.*'s systematic study on the depolymerization kinetics of head-to-tail (HT) PS, head-to-head (HH) PS, and a HT PS with one HH site. The HT PS with a single HH site depolymerizes PS at the fastest rate due to the facile initiation of one labile HH bond following the chain unzipping to styrene from the regioregular HT units along the backbone.[2–4,12] Since PS chains have primarily HT regiochemistry, which are harder to initiate than the HH bond as shown by previous density functional theory (DFT) methods, our approach post-functionalizes the PS backbone with multiple weak C–S bonds to form labile initiation sites for depolymerization, similar to the singly labile HH bond.[20] The most effective functionalization of PS for initiating depolymerization is a benzylic C–S bond since it has one of the lowest bond dissociation energy, aiding in the formation of the degradative centre for chain unzipping into monomer.[2–4,12,21,22] We hypothesize that benzylic C–S functionalization on the PS backbone will increase the rate of PS depolymerization, lower the depolymerization temperature, and improve the yield of styrene recovery (Fig. 1). To achieve this post-functionalization, we drew inspiration from prior work done by Xu *et al.*, which demonstrated the selective functionalization of benzylic C–H with a trifluoromethylthio (–SCF_3) functional group across a wide range of small-molecule drug derivatives.[23] We conducted a series of reaction optimizations to successfully adapt this small-molecule reaction to PS, which involved the following: (i) screening solvents that are concurrently compatible for photochemistry and the dissolution of PS, (ii) reducing side reactions, and (iii) polymer purification methods. With the successful synthesis and isolation of PS-SCF_3, we then observed a faster depolymerization rate and lower depolymerization temperature with PS-SCF_3 compared to pristine PS across a wide range of molecular weights. Notably, we achieved a greater styrene recovery from PS-SCF_3 compared to pristine PS across several consumer-grade samples (*i.e.*, PS food container, coffee lid, and red beverage cup). To our knowledge, this work is the first demonstration of the successful synthesis and isolation of PS-SCF_3 and its accelerated depolymerization relative to pristine PS.

Results

Synthesis of PS-SCF_3

Post-functionalization of PS with SCF_3 was achieved through systematic optimization of reaction solvent, base equivalence, and purification method. Solvent selection in photochemistry is governed by several criteria: the solvent must be photochemically inert, polar, aprotic, transparent across the UV-visible region, and possess a wide redox window.[24–26] For polymer substrates such as PS, solubility introduces an additional constraint, as PS is insoluble in solvents commonly employed in photochemical reactions (*e.g.*, acetonitrile, MeCN) and instead dissolves in apolar solvents (*e.g.*, 1,2-dichloroethane, cyclohexane).[27] Xu *et al.* reported optimal results with MeCN on a small-molecule substrate, while screening of dichloromethane, methanol, dimethylformamide, and tetrahydrofuran yielded only trace product, underscoring the sensitivity of photochemical reactions to solvent polarity and

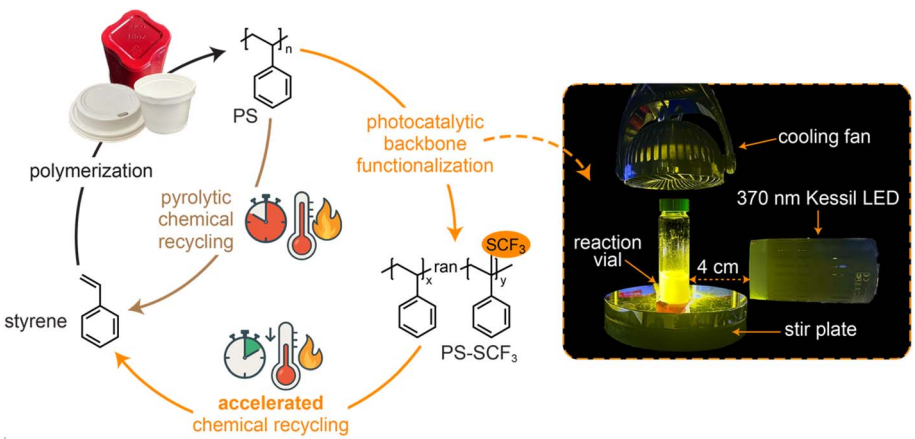

Fig. 1 Schematic of chemical recycling approaches for PS. Conventional pyrolysis requires high temperatures or longer timescales to recover styrene while post-functionalized PS-SCF_3 can recover styrene at lower temperatures and faster timescales. The photoreaction is set up in an N_2 glovebox with a 370 nm Kessil LED, cooling fan, and a stir plate.

redox window.[24] We screened solvents and solvent mixtures across a wide range of polarities on our small-molecule model system (*i.e.*, similar to the repeating styrene structure in the PS backbone), 2-(4-isopropylphenyl)-4,4,5,5-tetramethyl-1,3,2-dioxaborolane (referred to as isopropylbenzene-Bpin) as it enabled simpler structural analysis compared to PS samples. The broadness of PS proton peaks in nuclear magnetic resonance (NMR) spectroscopy makes definitive proton assignment challenging.[28,29] Product yields of isopropylbenzene-SCF_3-Bpin were determined *via* high-performance liquid chromatography coupled with electrospray ionization mass spectrometry using a linear calibration curve (Fig. S1–S4). Although MeCN provided the highest reaction yield of 34% (Fig. 2b, entry 1), MeCN is incapable of solubilizing PS. We therefore employed the second highest yielding solvent system, which was the binary solvent mixture of MeCN with 1,2-dichloroethane (1,2-DCE) in a 1 : 1 ratio (Fig. 2b, entry 14). This mixture offered a 23% reaction yield and became the solvent system used for the rest of this study.

The optimized trifluoromethylthiolation conditions established for isopropylbenzene-Bpin (Fig. 2b, entry 14) were applied directly to PS, and the crude polymer mixture was characterized by gel permeation chromatography (GPC). As PS does not absorb at the irradiation wavelength employed in the photoreaction, chain scission was not anticipated and was indeed absent in the GPC traces. Instead, a small increase in the molecular weight of the main PS peak was observed, consistent with successful SCF_3 functionalization of the PS backbone (Fig. S5). However, we observed undesirable crosslinking between polymer chains, primarily when post-functionalizing higher molecular weight PS (M_n > 50 kg mol^{-1}). We observed insoluble solids forming during the reaction and a higher number-averaged molecular weight (M_n) peak (at least twice the starting material's M_n, Fig. S5) *via* GPC. We postulate that the increase in M_n was due to the benzylic radicals on the PS backbone recombining between chains, in alignment with the proposed mechanism by Xu *et al.*[23] Experimentally, we found that a greater amount of base (*i.e.*, potassium carbonate, K_2CO_3) reduced the extent of crosslinking. Therefore, for all the subsequent studies, we decrease the equivalency of Phth-SCF_3 (1.3 to 0.1 equiv. Phth-SCF_3) and increased the amount of base (*i.e.*, 0.2 to 1.0 equiv. K_2CO_3) to reduce crosslinking (Fig. 2c).

To isolate PS-SCF_3 and enable independent assessment of the effect of –SCF_3 functionalization on depolymerization kinetics, purification of the crude polymer mixture was pursued. We initially attempted purification of PS-SCF_3 using conventional polymer purification techniques, such as precipitation, Soxhlet extraction, dialysis, and preparative recycling gel permeation chromatography (rGPC), but unexpectedly found an inseparable, yellow-colored impurity. The yellow, fluorescent impurity is untraceable *via* NMR (Fig. S6 and S7) but observable *via* ultraviolet-visible spectroscopy (UV-vis) (Fig. S9). We hypothesize this impurity to be the photocatalyst, 1,2,3,5-tetrakis(carbazol-9-yl)-4,6-dicyanobenzene (4CzIPN), based on its characteristic bright yellow color, abd prior reports of high 4CzIPN solubility in PS.[30] We found that the best purification came from normal-phase flash column chromatography, despite this technique rarely being used for polymer

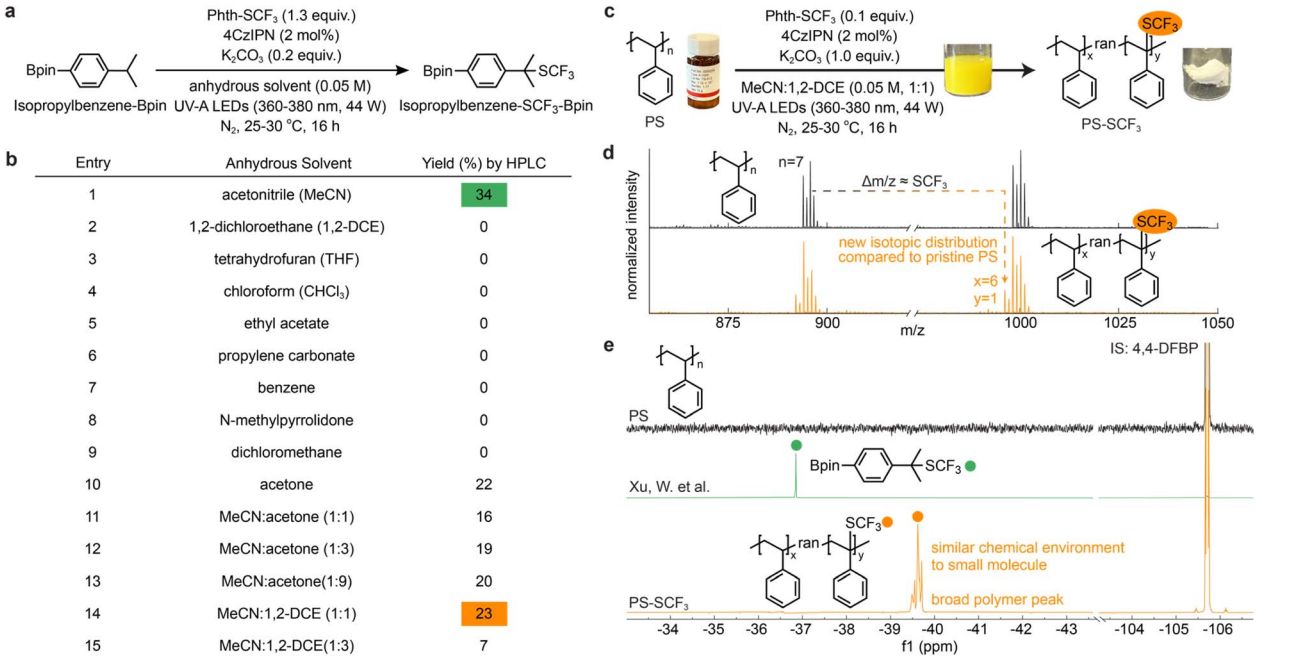

Fig. 2 (a) Reaction scheme of trifluoromethylthiolation on the small-molecule model system (isopropylbenzene-Bpin). (b) Table of the solvent optimization to solubilize PS. (c) Optimized reaction scheme of trifluoromethylthiolation on PS. (d) MALDI-TOF-MS spectra of PS-SCF_3, which shows an –SCF_3 substitution of the benzylic C–H. (e) ^{19}F NMR spectra of PS, isopropylbenzene-SCF_3-Bpin, and PS-SCF_3 which show polymer functionalization and similar chemical environment shifts. Phth-SCF_3 is 2-((trifluoromethyl)thio)isoindoline-1,3-dione, 4CzIPN is 1,2,3,5-tetrakis(carbazol-9-yl)-4,6-dicyanobenzene, LED is light-emitting diode, IS is internal standard, and 4,4-DFBP is 4,4-difluorobenzophenone.

purification as polymers are typically insoluble in solvents for normal-phase column chromatography and the conventional desire to purify polymers by size rather than polarity.[31,32] We determined that a solvent system of cyclohexane and ethyl acetate separated the impurity from PS-SCF_3 better than the other purification techniques, in terms of yield and purity (Fig. S9 and Table S3). Cyclohexane was selected as it is apolar and the theta solvent of PS.[33,34] We envision that purification could be circumvented by directly pyrolyzing the crude mixture, followed by collection of volatilized styrene *via* fractional distillation; however, this concept was not explored in this study as it adds complexity and we primarily sought to establish a baseline for the depolymerization of pure PS-SCF_3

To determine the successful synthesis of PS-SCF_3, we employed matrix-assisted laser desorption/ionization time-of-flight mass spectrometry (MALDI-TOF-MS), GPC analysis, and ^{19}F NMR spectroscopy (Fig. S24, 2S5 and S39). We analyzed a low M_n PS standard (PS-1.12K, $M_n = 1.12$ kg mol^{-1}) instead of a high M_n system ($M_n > 10$ kg mol^{-1}) because lower M_n PS can be precisely resolved by MALDI-TOF-MS to help confirm successful SCF_3-functionalization (Fig. 2d).[35] At high resolutions, MALDI-TOF-MS can detect the replacement of a proton with SCF_3 ($\Delta m/z = 100$ m/z) and new peaks will appear due to changes in isotopic distribution from the presence of SCF_3 (Fig. 2d). The MALDI-TOF-MS results align well with the GPC traces of PS-SCF_3 samples, showing an increase in M_n compared to pristine PS (Fig. S39). We cannot definitively confirm the regioselectivity of the –SCF_3 on the polymer backbone (*i.e.*, benzylic C–H *vs.* methylene C–H) due to the peak broadening of the alkyl peaks in the PS ^1H NMR spectra, as expected for polymeric samples.[28,29] However, we postulate that –SCF_3 is selectively functionalized on the benzylic position as we observe this with our small molecule analogue (Fig. 2a) using the same reaction conditions, which corroborates well with the substrate screening from Xu *et al.*[23] From ^{19}F NMR, two broad ^{19}F peaks at ~−40 ppm and ~−60 ppm were observed for the purified PS-SCF_3 samples (Fig. S12). The −40 ppm peak is attributed to the desired SCF_3-functionalization on the PS backbone as it is similar in chemical shift to the −37 ppm peak observed for our small-molecule model system (*i.e.*, isopropylbenzene-SCF_3-Bpin, Fig. 2e). To determine the identity of the −60 ppm fluorine peak, we designed a series of experiments on a dimer PS system (Table S4, Fig. S14–S23) to test the influence of water and oxygen, both potential deterrents in photochemical reactions.[36,37] We found that the additional fluorine peak is present regardless of the presence and/or absence of water and oxygen, but the presence of water significantly increases the intensity of the impurity peak from ^{19}F NMR (Fig. S12). We speculate that the ~−60 ppm impurity peak can be attributed to –OSO_2F or –$SCF_2(OH)$ based on its upfield ^{19}F NMR chemical shift and our results on a test dimeric PS system (*e.g.*, gas chromatography mass spectrometry (GC-MS) and direct analysis in real time mass spectrometry (DART-MS) results in Fig. S14–S23). Nevertheless, the backbone functionalization of –OSO_2F or –$SCF_2(OH)$ could decrease or increase the rate of depolymerization based on their respective bond strengths (C–O: 358 kJ mol^{-1}, C–S: 272 kJ mol^{-1}).[38]

Impact of SCF_3-functionalization on the depolymerization of PS-SCF_3

Thermogravimetric analysis (TGA) was employed to evaluate two metrics: (i) onset degradation temperature and (ii) total mass loss after 20 hours (Fig. 3a and b), providing a direct test of whether PS-SCF_3 depolymerizes at a faster rate and lower temperature than pristine PS.[39] Onset degradation temperature was determined by the intersection of extrapolated linear fits between the initial baseline and the tangent at the point of maximum gradient from dynamic TGA (ISO 11358-1, Fig. 3a).[40,41] Total mass loss was assessed isothermally at 300 °C (Fig. 3b) rather than at industrially typical temperatures above 400 °C because low temperatures offer improved safety and reduce formation of secondary byproducts[11,42] The improvements from SCF_3 functionalization are most pronounced in the lowest M_n PS-SCF_3 ($M_n = 1.12$ kg mol^{-1}, PS-1.12K-SCF_3), which achieved a six-fold increase in depolymerization rate (Fig. 3a) and a reduction in the onset degradation temperature from 350 °C to 323 °C relative to its pristine PS M_n analogue (Fig. 3b). The volatilized products from TGA contained styrene, benzene, and other related species (Fig. 3c) as detected by electron ionization MS, which suggest effective chain unzipping to monomers. Since SCF_3 functionalization offers labile initiation points, we can further accelerate depolymerization by increasing the number of SCF_3 units functionalized onto the PS backbone. The degree of functionalization is expressed as the mol% of SCF_3-functionalized styrene units relative to total styrene units, representing a sample-averaged quantity. For context, a 2 mol% functionalization corresponds to approximately 2 SCF_3 groups per PS chain at 10 kg mol^{-1}, but only 1 SCF_3 group per 5 chains at 1 kg mol^{-1}. To understand the trends of %SCF_3-functionalization, we synthesized two different % SCF_3-functionalizations of 1.7 mol% and 2.8 mol% by using different equivalents of Phth-SCF_3 (0.1 and 2 equivalents, respectively) on PS-1.12K (Fig. S55–S62 and Table S6). Dynamic TGA performed on the 1.7 mol% and 2.8 mol% SCF_3-functionalized samples confirmed that greater %SCF_3-functionalization lowered onset degradation temperatures by 20 °C and 27 °C relative to pristine PS, respectively. As for isothermal TGA, the 1.7 mol% and 2.8 mol% SCF_3-functionalized samples accelerated depolymerization by a greater mass loss of 17% and 34% compared to pristine PS, respectively (Fig. 3d, e, S63 and S64). Subsequently, we assessed our approach across a wide range of molecular weights (M_n = 1.12–110 kg mol^{-1}) that are representative of consumer-grade samples. At each molecular weight, we observed that PS-SCF_3 had an onset degradation temperature 10–20 °C lower compared to its pristine PS analogue and a greater mass loss of 10–35% over 20 hours (Fig. 3f and g).

To further understand the thermodynamics and kinetics of PS decomposition, we performed density functional theory calculations (DFT) on a proposed radical-based depolymerization mechanism consistent with prior literature[21,43,44] (Fig. S101), and the model-free isoconversional Flynn–Ozawa–Wall method (ASTM E1641). We calculated Gibbs free energy (ΔG) differences between the products, intermediates, transition states, and starting material for the potential initiation

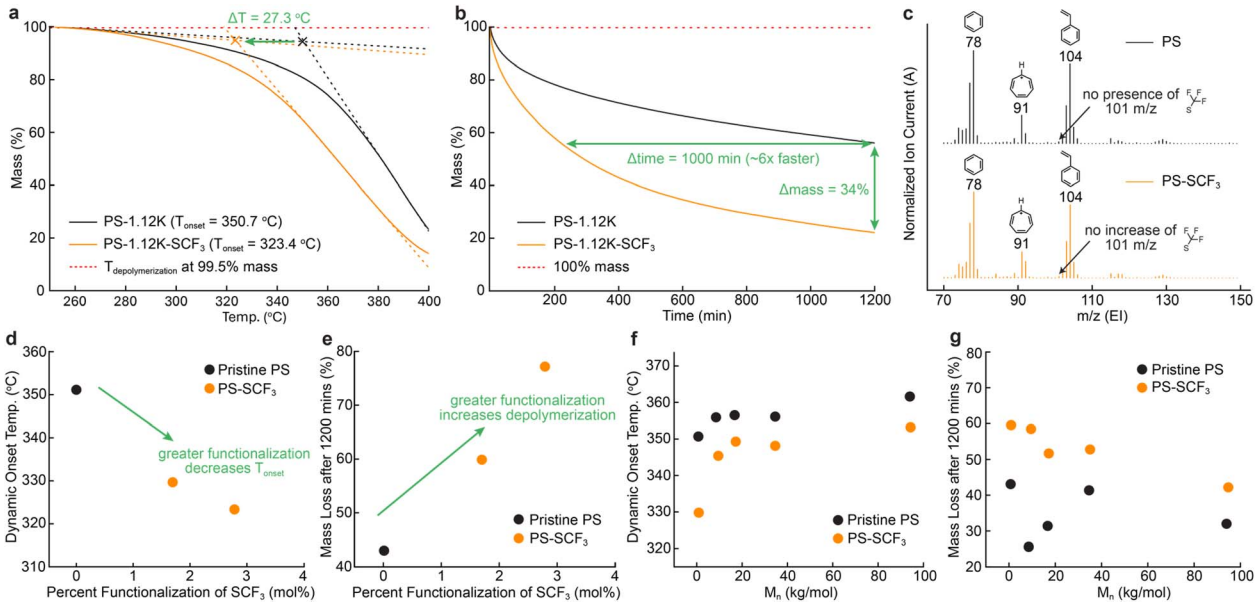

Fig. 3 (a) Dynamic TGA of PS-1.12K-SCF_3 compared with PS-1.12K. (b) Isothermal TGA at 300 °C for 20 h of PS-1.12K-SCF_3 compared with PS-1.12K. (c) Total ion current for each *m/z* across time over the isothermal TGA-MS at 300 °C for 20 h of PS-1.12K-SCF_3 compared with PS-1.12K which shows the detection of benzene, tropylium ion, and styrene and absence of SCF_3. (d) and (e) Percent SCF_3-functionalization study using PS-1.12K-SCF_3 on (d) onset temperature from dynamic TGA and (e) mass loss after 20 h from isothermal TGA. (f) and (g) Molecular weight study on (f) onset temperature from dynamic TGA and (g) mass loss after 20 h from isothermal TGA. The dashed lines are the linear trendlines for each molecular weight series.

pathways of PS and PS-SCF_3 were calculated (Fig. 4a). The small energy difference between states D and G reflects contributions from the other species present at each respective endpoint: ethylbenzene for D and $HSCF_3$ for G. The overall activation energy barrier is higher for pristine PS than for PS-SCF_3. Therefore, we propose that the increased depolymerization rate and lower onset degradation temperature observed for PS-SCF_3 arise from two cooperative effects: first, a relatively facile C–S homolytic fission for initiation (A, B *vs.* E, F, Fig. 4a); and second, more effective chain scission propagation by the SCF_3 radical (F, G, Fig. 4a) compared to the primary or secondary benzylic radicals generated by C–C homolytic fission in pristine PS (C, D, Fig. 4a). We used the Flynn–Ozawa–Wall analysis by running dynamic TGA experiments at different heating rates of 1 °C min^{-1}, 2 °C min^{-1}, 5 °C min^{-1}, and 10 °C min^{-1} on PS-10K and PS-10K-SCF_3 (Fig. 4b and d) to determine the apparent activation energy (E_a) of degradation at specific conversion points (Fig. 4c and e). We evaluated conversions between 10 and 20% because we wanted to avoid early loss of volatile impurities while also investigating early degradation pathways, which we speculate would involve more initiation events than main chain unzipping.[45,46] On average, the degradation of PS-10K-SCF_3 had an E_a that is 11 kJ mol^{-1} lower compared to PS-10K, which further supports our findings of the accelerated depolymerization of PS-SCF_3 relative to pristine PS (Fig. 4f). In addition, we observe that as the conversion increases, the E_a decreases, which suggests a complex, multi-step degradation mechanism indicative of greater proportion of main chain unzipping from already initiated chains rather than the initiation of new chains.

Pyrolysis of PS-SCF_3 under positive flow of argon

To benchmark our protocol, we quantified the yield of styrene from the pyrolysis of consumer-grade PS and PS-SCF_3 samples. We post-functionalized six different consumer-grade PS samples for pyrolysis, which were obtained from local stores (Fig. S65–S88 and Table S7). We observed a lower onset degradation temperature for three of the six SCF_3-functionalized samples (PS food container, coffee lid, and red beverage cup) compared to its unfunctionalized counterpart (Fig. S96, S98 and S100) while the other SCF_3-functionalized Styrofoam peanuts, Petri dishes, and blue cups had a higher onset degradation temperature compared to its unfunctionalized counterpart (Fig. S90, S92 and S94). The inconsistent behavior of consumer-grade PS samples is attributed to uncharacterized variables inherent to commercial formulations, most notably differences in polymer architecture and proprietary additives, which may inhibit depolymerization. We therefore focused subsequent pyrolysis experiments on the three consumer-grade samples whose onset degradation temperatures fell below that of unfunctionalized PS. The PS standard of $M_n = 110$ kg mol^{-1} was selected as a benchmark PS sample because its molecular weight was closest to consumer-grade samples. Each sample was heated to 300 °C for 20 hours under a positive flow of Argon, and the product feed was subsequently trapped in a collection vial containing DMSO-d_6 (Fig. 5a). Each sample was compared against a known amount of internal standard, 1,3,5-trimethoxybenzene, to quantify the styrene yield in the collection vial, the transfer cannula, and the reaction vial (Fig. 5b and S108–S119) using ^{1}H NMR. The PS-SCF_3 standard (M_n = 110 kg mol^{-1}) and consumer-grade PS-SCF_3 samples consistently produced higher styrene yields compared to their

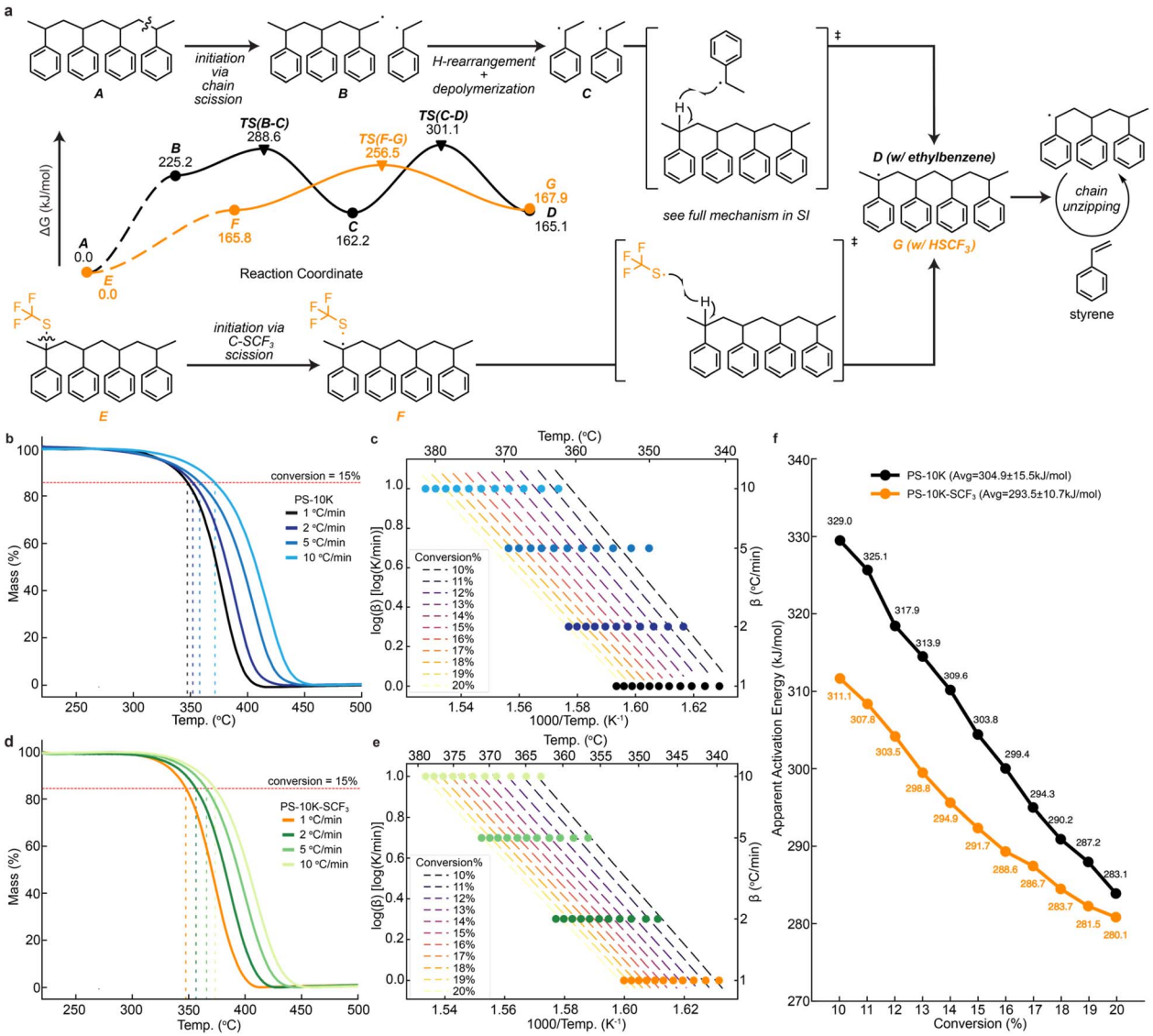

Fig. 4 (a) Proposed mechanism on a tetrameric model system for comparing the Gibbs free energy (Δ*G*) of the initiation and propagation of PS and PS-SCF_3 to form the degradative centre necessary for chemical recycling to styrene. (b) Dynamic TGA of PS-10K at different heating rates (β = 1 °C min^{-1}, 2 °C min^{-1}, 5 °C min^{-1}, and 10 °C min^{-1}) for the Flynn–Ozawa–Wall analysis. 10% conversion is shown as an example for extracting the temperature at specific conversions across different heating rates. (c) Plot of log(β) *vs.* 1000/*T* for PS-10K to estimate the apparent activation energy (E_a) at each conversion% between 5% and 15%. (d) Dynamic TGA of PS-10K-SCF_3 at different heating rates (1 °C min^{-1}, 2 °C min^{-1}, 5 °C min^{-1}, and 10 °C min^{-1}) for the Flynn–Ozawa–Wall analysis. (e) Plot of log(β) *vs.* 1000/*T* for PS-10K-SCF_3 to estimate the apparent activation energy (E_a) from the slope at each conversion% between 5% and 15%. (f) Comparison of the apparent activation energy at each conversion between PS-10K and PS-10K-SCF_3.

unfunctionalized counterparts. The functionalized samples (PS-SCF_3 standard, PS food container, PS coffee lid, and red beverage cup) yielded styrene recover of 28.5%, 24.8%, 10.7%, and 16.3%, respectively, compared to 24.4%, 21.6%, 6.3%, and 7.9% for the corresponding unfunctionalized samples which corroborates well with the trends from our isothermal TGA results (Fig. 5c, S53, S95, S97 and S99). However, the collected styrene yields in the distillation apparatus are lower than the TGA analysis. We mainly attribute this discrepancy to the fact that the collected products from distillation measures styrene yield while TGA measures mass loss. In addition, the distillation setup resulted in volatilization losses from imperfect collection due to the positive flow of Argon gas and long reaction times (20 hours) in the collection flask. For the PS-SCF_3 samples, we observed trace amounts of fluorinated byproducts in the collection vial from ^{19}F NMR which could be a potential hazard. For future use cases, fractional distillation could be employed to purify and capture the byproducts. Unexpectedly, the red dye additive in the red beverage cup did not prevent the photochemical post-functionalization as the red dye degrades under UV irradiation,[47] which allowed for successful SCF_3 functionalization and subsequent depolymerization. Our post-functionalization approach demonstrated effective chemical recycling of these consumer-grade materials even without significant optimization or detailed knowledge of their processing history and additive composition.

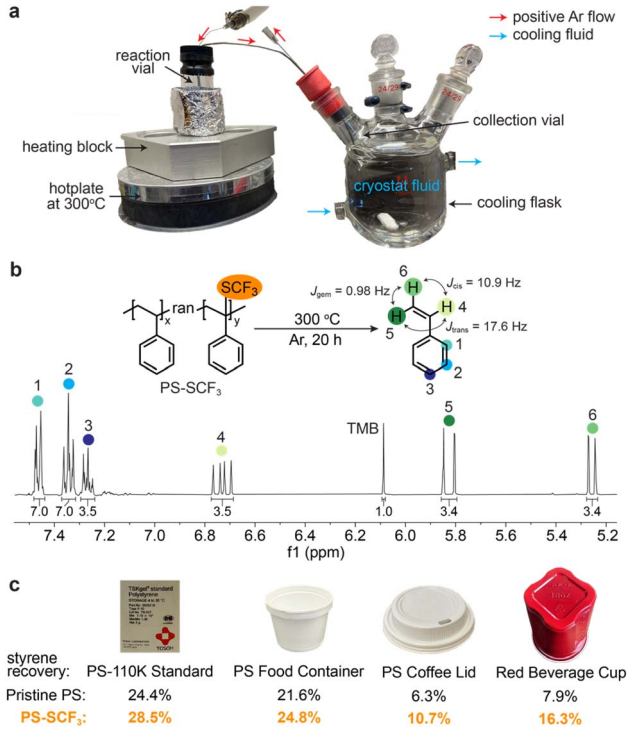

Fig. 5 (a) Diagram of distillation apparatus. (b) ^{1}H NMR spectra of collected styrene and internal standard for quantification. (c) Consumer-grade PS and PS-SCF_3 samples undergo pyrolysis at 300 °C over 20 h with styrene % yield.

Conclusions and outlook

In this work, we have developed a proof-of-concept method to accelerate the chemical recycling of PS by post-functionalizing labile –SCF_3 groups onto an otherwise inert PS backbone. Across a range of molecular weights and consumer-grade samples, we demonstrate PS-SCF_3 has improved depolymerization kinetics and a greater recovery of styrene compared to pristine PS. Subsequent studies will investigate alternative labile functional groups capable of further reducing the depolymerization activation energy, with an emphasis on minimizing cost and toxicity hazards. Industry collaboration for pyrolysis scale-up in tandem with understanding processing methods and additives used for PS is necessary to meaningfully translate this work to consumer-grade PS products. Overall, the post-functionalization design strategy described within this study establishes a compelling approach to post-functionalize consumer-grade PS and chemically recycle PS at lower temperatures and faster timescales. We hope this work will inspire others to adopt a similar approach and enable access to the vast quantities of existing plastic waste as a monomeric feedstock.

Author contributions

S. L. and H. T. conceptualized this work. S. L. and A. L. designed the experiments. S. L. carried out all the experiments and A. L. helped with some of the purification and TGA measurements. C. T. S. performed the DFT calculations. A. A. G. and H. T. supervised and acquired funds for the research. S. L. wrote the article – original draft. All the authors contributed to the discussion and paper revision.

Conflicts of interest

A. A. G. is an employee of NVIDIA.

Data availability

Experimental data associated with this work are available in the supplementary information (SI). Additional data is available from the corresponding authors upon request. From the DFT calculations, computed structures and energies are available on https://iochem-bd.matter.toronto.edu. Search for "styrene" and "tetramer" to find the relevant information. Supplementary information: extensive raw data (UV-Vis, GPC, NMR, TGA) and discussion on the solvent screening, purification comparisons, full DFT mechanistic calculations, Flynn–Ozawa–Wall analysis, and pyrolysis product quantification. See DOI: https://doi.org/10.1039/d6sc03696a.

Acknowledgements

S. L. would like to thank the CSICOMP NMR Facility, Dr Darcy Burns, and Dr Sherry Dai for help with NMR analysis; Dr Eloi Grignon, Ebad Noman, Prof. Dwight Seferos for help with TGA analysis; Dr Victor Lotocki, Kimia Hosseini, Prof. Dwight Seferos for access to GPC analysis; Dr Matthew Forbes and the AIMS Mass Spectrometry Laboratory for help with MALDI-TOF-MS and DART-MS analysis; Dr Jared Mudrik and ANALEST for help with GC-MS analysis; Prof. Felix Strieth-Kalthoff, Dr Han Hao, and Dr Yang Cao for their help with general synthesis advice; Dr Rachel Keunen and Jingbang Liang for help with general chemistry equipment and lab management; Prof. Varinia Bernales for their assistance in the DFT protocol; and Chris Crebolder for the maintenance of computing resources. This research was enabled in part by support provided by Compute Ontario (https://www.computeontario.ca) and the Digital Research Alliance of Canada (https://www.alliancecan.ca). S. L. and A. L. acknowledges the support by the Natural Sciences and Engineering Research Council (NSERC) of Canada through the post-graduate doctoral scholarship. S. L. and C. T. S. acknowledges the support by the Vector Institute for Artificial Intelligence. A. A.-G. thanks Anders G. Frøseth for his generous support. A. A.-G. acknowledges funding by Natural Resources Canada and the Canada 150 Research Chairs program. A. A.-G. and H. T. acknowledges funding by the Acceleration Consortium, which receives funding from the CFREF-2022-00042 Canada First Research Excellence Fund. A. A.-G. acknowledges funding by the US Office of Naval Research (Award No. #N000142112137).

References

1 A. H. Tullo, Plastic has a problem; is chemical recycling the solution?, *Chem. Eng. News*, 2019, **97**(39).

2 B. A. Howell, Y. Cui and D. B. Priddy, Assessment of the thermal degradation characteristics of isomeric poly(styrene)s using TG, TG/MS and TG/GC/MS, *Thermochim. Acta*, 2003, **396**(1), 167–177, DOI: 10.1016/S0040-6031(02)00522-1.
3 B. A. Howell and K. Chaiwong, Thermal stability of poly(styrene) containing no head-to-head units, *J. Therm. Anal. Calorim.*, 2009, **96**(1), 219–223, DOI: 10.1007/s10973-005-7336-x.
4 B. a. Howell, Y. Cui, K. Chaiwong and H. Zaho, Polymerization as a means of stabilization for polystyrene, *J. Vinyl Addit. Technol.*, 2006, **12**(4), 198–203, DOI: 10.1002/vnl.20091.
5 Y. Xu and W. Schrader, Trash-to-fuel: Converting municipal waste into transportation fuels by pyrolysis, *iScience*, 2022, **25**(4), 104036, DOI: 10.1016/j.isci.2022.104036.
6 M. M. Hasan, R. Haque, M. I. Jahirul and M. G. Rasul, Pyrolysis of plastic waste for sustainable energy Recovery: Technological advancements and environmental impacts, *Energy Convers. Manage.*, 2025, **326**, 119511, DOI: 10.1016/j.enconman.2025.119511.
7 J. Li, D. Yu, L. Pan, X. Xu, X. Wang and Y. Wang, Recent advances in plastic waste pyrolysis for liquid fuel production: critical factors and machine learning applications, *Appl. Energy*, 2023, **346**, 121350, DOI: 10.1016/j.apenergy.2023.121350.
8 Polymer Data Handbook ISO-11358-1-2022, 2022.
9 D. E. Roberts, Heats of polymerization – a summary of published values and their relation to structure, *J. Res. Natl. Bur. Stand.*, 1950, **44**(3), 221, DOI: 10.6028/jres.044.021.
10 G. R. Jones, H. S. Wang, K. Parkatzidis, R. Whitfield, N. P. Truong and A. Anastasaki, Reversed Controlled Polymerization (RCP): Depolymerization from Well-Defined Polymers to Monomers, *J. Am. Chem. Soc.*, 2023, **145**(18), 9898–9915, DOI: 10.1021/jacs.3c00589.
11 C. Marquez, C. Martin, N. Linares and D. D. Vos, Catalytic routes towards polystyrene recycling, *Mater. Horiz.*, 2023, **10**(5), 1625–1640, DOI: 10.1039/d2mh01215d.
12 B. A. Howell, The Mechanism of Poly(Styrene) Degradation, in *Reactions and Mechanisms in Thermal Analysis of Advanced Materials*, John Wiley & Sons, Ltd, 2015, p. 259–267, available from: https://onlinelibrary.wiley.com/doi/abs/10.1002/9781119117711.ch11, DOI: 10.1002/9781119117711.ch11.
13 I. M. Maafa, Pyrolysis of Polystyrene Waste: A Review, *Polymers*, 2021, **13**(2), 2, DOI: 10.3390/polym13020225.
14 Y. S. Kim, G. C. Hwang, S. Y. Bae, S. C. Yi, S. K. Moon and H. Kumazawa, Pyrolysis of polystyrene in a batch-type stirred vessel, *Korean J. Chem. Eng.*, 1999, **16**(2), 161–165, DOI: 10.1007/BF02706830.
15 Z. Zhang, T. Hirose, S. Nishio, Y. Morioka, N. Azuma, A. Ueno, *et al.*, Chemical Recycling of Waste Polystyrene into Styrene over Solid Acids and Bases, *Ind. Eng. Chem. Res.*, 1995, **34**(12), 4514–4519, DOI: 10.1021/ie00039a044.
16 V. Kumar, A. Khan and M. Rabnawaz, Efficient Depolymerization of Polystyrene with Table Salt and Oxidized Copper, *ACS Sustainable Chem. Eng.*, 2022, **10**(19), 6493–6502, DOI: 10.1021/acssuschemeng.1c08400.
17 J. Doucet, J. P. Laviolette, S. Farag and J. Chaouki, Distributed Microwave Pyrolysis of Domestic Waste, *Waste Biomass Valorization*, 2014, **5**(1), 1–10, DOI: 10.1007/s12649-013-9216-0.
18 S. Oh, H. Jiang, L. H. Kugelmass and E. E. Stache, Recycling of Post-Consumer Waste Polystyrene Using Commercial Plastic Additives, *ACS Cent. Sci.*, 2025, **11**(1), 57–65, DOI: 10.1021/acscentsci.4c01317.
19 J. B. Young, J. I. Bowman, M. E. Lott, L. A. Diodati, K. C. Stevens, R. W. Hughes, *et al.*, Bulk Depolymerization of Polystyrene with Comonomer Radical Triggers, *ACS Macro Lett.*, 2025, **14**(5), 576–581, DOI: 10.1021/acsmacrolett.5c00159.
20 J. Huang, X. Li, H. Meng, H. Tong, X. Cai and J. Liu, Studies on pyrolysis mechanisms of syndiotactic polystyrene using DFT method, *Chem. Phys. Lett.*, 2020, **747**, 137334, DOI: 10.1016/j.cplett.2020.137334.
21 M. L. Poutsma, Mechanistic analysis and thermochemical kinetic simulation of the pathways for volatile product formation from pyrolysis of polystyrene, especially for the dimer, *Polym. Degrad. Stab.*, 2006, **91**(12), 2979–3009, DOI: 10.1016/j.polymdegradstab.2006.08.015.
22 S. W. Benson, III – Bond energies, *J. Chem. Educ.*, 1965, **42**(9), 502, DOI: 10.1021/ed042p502.
23 W. Xu, W. Wang, T. Liu, J. Xie and C. Zhu, Late-stage trifluoromethylthiolation of benzylic C-H bonds, *Nat. Commun.*, 2019, **10**(1), 4867, DOI: 10.1038/s41467-019-12844-9.
24 M. A. Bryden, F. Millward, O. S. Lee, L. Cork, M. C. Gather, A. Steffen, *et al.*, Lessons learnt in photocatalysis – the influence of solvent polarity and the photostability of the photocatalyst, *Chem. Sci.*, 2024, **15**(10), 3741–3757, DOI: 10.1039/d3sc06499a.
25 R. H. Verschueren and W. M. De Borggraeve, Electrochemistry and Photoredox Catalysis: A Comparative Evaluation in Organic Synthesis, *Molecules*, 2019, **24**(11), 2122, DOI: 10.3390/molecules24112122.
26 R. K. Venkatraman and A. J. Orr-Ewing, Solvent Effects on Ultrafast Photochemical Pathways, *Acc. Chem. Res.*, 2021, **54**(23), 4383–4394, DOI: 10.1021/acs.accounts.1c00549.
27 M. T. García, I. Gracia, G. Duque, A. d. Lucas and J. F. Rodríguez, Study of the solubility and stability of polystyrene wastes in a dissolution recycling process, *Waste Manage.*, 2009, **29**(6), 1814–1818, DOI: 10.1016/j.wasman.2009.01.001.
28 K. Hatada and T. Kitayama, *NMR Spectroscopy of Polymers*, Springer Berlin Heidelberg, Berlin, Heidelberg, 2004, available from: https://link.springer.com/10.1007/978-3-662-08982-8 doi:DOI: 10.1007/978-3-662-08982-8.
29 J. E. Mark. *Physical properties of polymers handbook*, Springer, New York, 2nd edn, 2007.
30 A. J. Gillett, A. Pershin, R. Pandya, S. Feldmann, A. J. Sneyd, A. M. Alvertis, *et al.*, Dielectric control of reverse intersystem crossing in thermally activated delayed fluorescence

emitters, *Nat. Mater.*, 2022, **21**(10), 1150–1157, DOI: 10.1038/s41563-022-01321-2.

31 J. Lawrence, E. Goto, J. M. Ren, B. McDearmon, D. S. Kim, Y. Ochiai, *et al.*, A Versatile and Efficient Strategy to Discrete Conjugated Oligomers, *J. Am. Chem. Soc.*, 2017, **139**(39), 13735–13739, DOI: 10.1021/jacs.7b05299.

32 J. Lawrence, S. H. Lee, A. Abdilla, M. D. Nothling, J. M. Ren, A. S. Knight, *et al.*, A Versatile and Scalable Strategy to Discrete Oligomers, *J. Am. Chem. Soc.*, 2016, **138**(19), 6306–6310, DOI: 10.1021/jacs.6b03127.

33 G. Jones and D. Caroline, Intramolecular motion of polystyrene in K theta solvent, *Chem. Phys. Lett.*, 1978, **58**(1), 149–152.

34 S. Rasouli, M. R. Moghbeli and S. J. Nikkhah, A deep insight into the polystyrene chain in cyclohexane at theta temperature: molecular dynamics simulation and quantum chemical calculations, *J. Mol. Model.*, 2019, **25**(7), 195, DOI: 10.1007/s00894-019-4078-4.

35 M. E. Payne and S. M. Grayson, Characterization of Synthetic Polymers *via* Matrix Assisted Laser Desorption Ionization Time of Flight (MALDI-TOF) Mass Spectrometry, *J. Visualized Exp.*, 2018, **10**(136), 57174, DOI: 10.3791/57174.

36 A. A. Abdel-Shafi and D. R. Worrall, Mechanism of the excited singlet and triplet states quenching by molecular oxygen in acetonitrile, *J. Photochem. Photobiol., A*, 2005, **172**(2), 170–179, DOI: 10.1016/j.jphotochem.2004.12.006.

37 J. Giaimuccio, M. Zamadar, D. Aebisher, G. J. Meyer and A. Greer, Singlet Oxygen Chemistry in Water. 2. Photoexcited Sensitizer Quenching by O2 at the Water—Porous Glass Interface, *J. Phys. Chem. B*, 2008, **112**(49), 15646–15650, DOI: 10.1021/jp807556x.

38 J. E. Huheey, E. A. Keiter, R. L. Keiter and O. K. Medhi, *Inorganic chemistry: principles of structure and reactivity*, Pearson, New Delhi, 4th edn, 2013.

39 C. David, Chapter 1 Thermal Degradation of Polymers, in *Comprehensive Chemical Kinetics*, ed. Bamford C. H. and Tipper C. F. H., Elsevier, 1975, pp. 1–173, (Degradation of Polymers), available from: https://www.sciencedirect.com/science/article/pii/S0069804008703339, DOI: 10.1016/S0069-8040(08)70333-9.

40 E37 Committee. *Test Method for Thermal Stability by Thermogravimetry*, ASTM International, [cited 2025 Oct 2], available from: http://www.astm.org/cgi-bin/resolver.cgi?E2550-11, DOI: 10.1520/E2550-11.

41 Polymer Data Handbook ISO-11358-1-2022, 2022.

42 S. D. Anuar Sharuddin, F. Abnisa, W. M. A. Wan Daud and M. K. Aroua, A review on pyrolysis of plastic wastes, *Energy Convers. Manage.*, 2016, **115**, 308–326, DOI: 10.1016/j.enconman.2016.02.037.

43 T. M. Kruse, O. S. Woo, H. W. Wong, S. S. Khan and L. J. Broadbelt, Mechanistic Modeling of Polymer Degradation: A Comprehensive Study of Polystyrene, *Macromolecules*, 2002, **35**(20), 7830–7844, DOI: 10.1021/ma020490a.

44 T. Faravelli, M. Pinciroli, F. Pisano, G. Bozzano, M. Dente and E. Ranzi, Thermal degradation of polystyrene, *J. Anal. Appl. Pyrolysis*, 2001, **60**(1), 103–121, DOI: 10.1016/S0165-2370(00)00159-5.

45 E37 Committee, *Test Method for Decomposition Kinetics by Thermogravimetry Using the Ozawa/Flynn/Wall Method*, ASTM International, [cited 2025 Nov 14], available from: http://www.astm.org/cgi-bin/resolver.cgi?E1641-23, DOI: 10.1520/E1641-23.

46 S. Vyazovkin, A. K. Burnham, J. M. Criado, L. A. Pérez-Maqueda, C. Popescu and N. Sbirrazzuoli, ICTAC Kinetics Committee recommendations for performing kinetic computations on thermal analysis data, *Thermochim. Acta*, 2011, **520**(1), 1–19, DOI: 10.1016/j.tca.2011.03.034.

47 C. Boyles and S. J. S. Sobeck, Photostability of organic red food dyes, *Food Chem.*, 2020, **315**, 126249, DOI: 10.1016/j.foodchem.2020.126249.